



Cyclic voltammetric determination of phosphate in tap water via [Omim]₆Mo₇O₂₄-carbon paste electrodes

Jialin Zhou¹ · Jiayu Fei¹ · Cheng Zeng² · Hong Hua Quan¹ · Ming Li¹

Received: 12 January 2023 / Accepted: 31 May 2023 / Published online: 9 June 2023
© Institute of Chemistry, Slovak Academy of Sciences 2023

Abstract

Stably retaining the water-soluble molybdate within electrodes is of great significance in phosphate analysis. This study fabricated an [Omim]₆Mo₇O₂₄ carbon paste electrode (OCPE), which was able to effectively retain molybdate in the aqueous solution. The electrochemistry of phosphate at the surface of the OCPE was studied using cyclic voltammetry (CV). The voltammograms showed three reversible redox peaks corresponding to the redox of Mo(VI/V) as well as several irreversible peaks involving the formation of hydrogen molybdenum bronze. The currents of all three reversible redox peaks linearly varied versus phosphate concentrations in 0.1 mol·L⁻¹ H₂SO₄-KCl. After optimizing the mass ratio of the [Omim]₆Mo₇O₂₄ and carbon powder, peak C6 shows a wide linear range (1.0 × 10⁻²–1.0 × 10⁻⁷ mol·L⁻¹; R² = 0.9970) with a sensitivity of 5.3 (± 0.1) μA/μM. The limit of detection (LOD = 3σ/s) was 8.5 × 10⁻⁸ mol·L⁻¹. Interferences from common anions, silicate, and glyphosate on phosphate analysis were also investigated. The proposed sensing method was successfully applied to the determination of phosphate in tap water, whose results were verified with ion chromatography (IC).

Keywords [Omim]₆Mo₇O₂₄ electrodes · Phosphate analysis · Tap water · Cyclic voltammetry

Introduction

Determination of inorganic phosphate is important for environmental and life science applications (Macintosh et al. 2018; Ellam and Chico 2012). Therefore, there is an ongoing interest in both environmental researchers and bioanalytical chemists to develop simple, sensitive, and cost-effective approaches for phosphate analysis. Various analytical techniques have been developed to analyze the concentration of phosphate in environmental, industrial, clinical, and biological samples including ion chromatography with capillary electrophoresis, (Ruiz-Calero and Galceran 2005; Chang et al. 2005) colorimetry, (Yan et al. 2019; Liu et al. 2013; He et al. 2013) optical fluorescence, (Nagaraj et al. 2021; Zhang et al. 2022) spectrophotometry, (Snigur et al. 2020; Clinton-Bailey et al. 2017) and electrochemistry (Forano et al. 2018).

Electrochemical methods have several advantages over other techniques including good detection sensitivity, selectivity, high throughput, miniaturization, cost-effectiveness, adaptability, and suitability for field measurements. Other than potentiometric methods, the most popular electroanalytical method for the determination of phosphate involves the treatment of the sample with an acidic molybdate solution to convert the phosphate into the Keggin anions (PMo₁₂O₄₀³⁻), with subsequent electrochemical reduction leading to mixed molybdenum oxidation state (Nagul et al. 2015). The use of direct electroreduction techniques can lead to portability and excellent sensitivity, which make them very attractive for on-site monitoring of phosphate.

In general, the source of Mo used for the electrochemical phosphate detection is water-soluble salts such as Na₂MoO₄ (VI) and (NH₄)₆Mo₇O₂₄ (VI) even when the reaction must occur on the surface of an electrode rather than in solution. Hence, the preparation of electrodes requires one to stably retain the water-soluble molybdate in an aqueous solution. Multiple papers have reported on the preparation or modification of electrodes with molybdenum sources utilizing a range of different materials such as graphite inks, (Lu et al. 2021a) carbon black nanoparticles, (Kumar et al. 2021) poly (vinyl chloride), (Kolliopoulos et al. 2015; Talarico

✉ Ming Li
liming@yzu.edu.cn

¹ College of Environmental Science and Engineering,
Yangzhou University, Yangzhou 225127,
People's Republic of China

² Yangzhou Customs District, Yangzhou 225000,
People's Republic of China

et al. 2015) poly(vinylidene fluoride-co-hexafluoropropylene, (Cinti et al. 2016) chitosan ionic-liquid hybrid matrix, (Berchmans et al. 2011) and zirconium dioxide/zinc oxide/multiple-wall carbon nanotubes (Lu et al. 2021b) to achieve superior analytical performance for the phosphate analysis. An electrochemical sensor was prepared via zirconium dioxide, zinc oxide, multiple-wall carbon nanotubes, ammonium molybdate tetrahydrate, and a screen-printed electrode. This sensor was used to explore the electro-redox reaction of phosphomolybdate complexes on the surface of the electrode, thus resulting in a lower detection limit ($\text{LOD}=2.0 \times 10^{-8} \text{ mol L}^{-1}$). (Lu et al. 2021b) However, most phosphomolybdate-based methods that use voltammetry are commonly accompanied by tedious fabrication with the electrode decorated via nanomaterials to increase sensitivity. Therefore, phosphate-measuring electrodes with a simple fabrication method are always desirable.

Recently, we reported on the synthesis of $[\text{Omim}]_6\text{Mo}_7\text{O}_{24}$ and its application in potentiometric PF_6^- ion sensors. (Shi et al. 2021) Here, we fabricate $[\text{Omim}]_6\text{Mo}_7\text{O}_{24}$ -carbon paste electrodes (OCPEs) and apply them to the determination of phosphate in tap water.

Experimental

Materials

Chemicals

The 1-octyl-3-methylimidazolium chloride ($\geq 97\%$), ammonium molybdate tetrahydrate (AR), silicone oil (10 mPa·s,

25 °C), carbon powder (3000 mesh), sodium dihydrogen phosphate anhydrous ($\geq 99\%$), and potassium chloride ($\geq 99\%$) were purchased from Shanghai Aladdin Biochemical Technology Co., Ltd. Potassium hydroxide ($\geq 95\%$), sulfuric acid, and hydrochloric acid were obtained from Sinopharm Chemical Reagent Co., Ltd. All chemicals were used as received without additional purification. All solutions were prepared with water purified in a Milli-Q System (Millipore, Bedford, MA, USA).

The phosphate standard solution was prepared as follows: The KCl electrolyte (0.7455 g) was dissolved in 100 mL of $0.1 \text{ mol}\cdot\text{L}^{-1}$ sulfuric acid solution to obtain $0.1 \text{ mol}\cdot\text{L}^{-1}$ H_2SO_4 -KCl mixed solution. We then weighed 0.1380 g sodium dihydrogen phosphate monohydrate and added it to 10.0 mL of the above-mixed solution. The solution was stirred and vibrated fully to dissolve it and obtain $0.10 \text{ mol}\cdot\text{L}^{-1}$ phosphate stock solution. We then used a pipette to transfer 1.0 mL of phosphate stock solution into another test tube and added 9.0 mL of $0.10 \text{ mol}\cdot\text{L}^{-1}$ H_2SO_4 -KCl mixed solution to obtain $1.0 \times 10^{-2} \text{ mol}\cdot\text{L}^{-1}$ phosphate stock solution. This process was repeated to obtain a series of 1.0×10^{-2} – $1.0 \times 10^{-8} \text{ mol}\cdot\text{L}^{-1}$ phosphate standard solutions.

Apparatus

Voltammetric measurements were collected using a CHI800D electrochemical analyzer (Shanghai Chenhua Instrument Co., Ltd.) with an Ag/AgCl reference electrode (CHI111) and a Pt wire counter electrode (CHI115) connected to a laptop (Fig. 1). A digital magnetic stirrer (HS501, IKA, Guangzhou, China) and clinical centrifuge

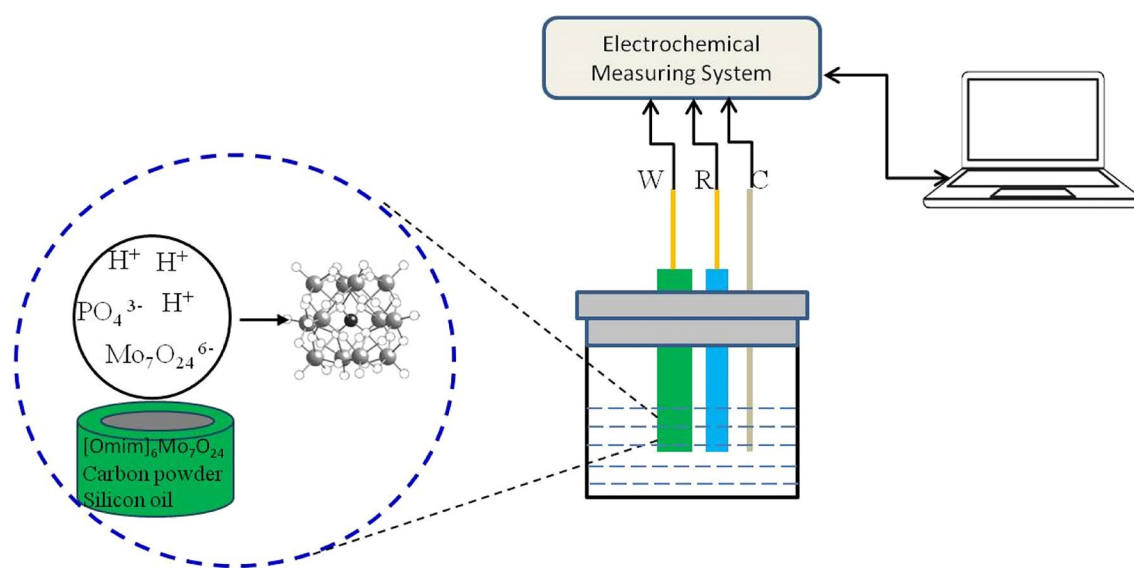


Fig. 1 Schematic diagram of experimental device

(L420-A, Cence, Hunan Changsha, China) were used for $[\text{Omim}]_6\text{Mo}_7\text{O}_{24}$ synthesis. Metrohm 883 IC + ion chromatography verified the phosphate concentration in tap water.

Synthesis of $[\text{Omim}]_6\text{Mo}_7\text{O}_{24}$

$[\text{Omim}]_6\text{Mo}_7\text{O}_{24}$ was synthesized according to the literature Shi et al. (2021). Briefly, 20 mL of $50 \text{ mmol}\cdot\text{L}^{-1}$ 1-octyl-3-methylimidazolium chloride solution was added dropwise into a 100-mL beaker pre-loaded with 20 mL of $50 \text{ mmol}\cdot\text{L}^{-1}$ ammonium molybdate solution. This was stirred at room temperature for 30 min. The resulting white suspension was centrifuged at $4000 \text{ r}\cdot\text{min}^{-1}$ for 20 min and washed with small amounts of water until no chloride impurities could be detected by the silver nitrate test. The final milky white solid was dried in vacuum at $60 \text{ }^\circ\text{C}$ for 4 h, followed by ball milling with an agate mortar by hand to obtain a homogeneous paste around micron-sizes.

Preparation of OCPE

We started with a beaker containing 255 mg of carbon powder and 50 mg of silicon oil and then, added different quantities of $[\text{Omim}]_6\text{Mo}_7\text{O}_{24}$ with mass ratios of 0, 5%, 10%, 15%, and 20%. After mixing for 30 min at room temperature, the homogeneous slurry was distributed into an ϕ 4.0-mm plastic syringe with the syringe rod under hand-pressure. An extrinsic electrical junction was approved by enforcing a copper wire down the syringe, which was followed by polishing the CPE surface with 1000-, 4000-, and 8000-mesh SiC abrasive papers to obtain an OCPE. This was then left to dry overnight at room temperature.

Characteristics of OCPE

Scanning electron micrographs (SEMs) were collected with an S-4800II field emission scanning electron microscope (Hitachi, Japan) equipped with Noran EDS (Thermo Electron Corporation) to obtain morphological characteristics of OCPE. The XPS spectrum of the surface layer was obtained using ESCALAB250Xi model (Thermo Fisher Scientific, USA) to confirm the molybdenum species on the OCPE surface layer.

Experimental conditions

The OCPE working electrode (WE), platinum wire counter electrode (CE), and $\text{Ag}/\text{AgCl}/\text{KCl}$ ($3 \text{ mol}\cdot\text{L}^{-1}$) reference electrode (RE) were connected to the electrochemical workstation. CV was initially performed in 10 mL of supporting electrolyte solution consisting of $0.1 \text{ mol}\cdot\text{L}^{-1}$ H_2SO_4 -KCl (volume ratio of 1:1) mixed solution under an operating potential range of -0.4 – 1.2 V vs. SCE.

Sample measurements

The samples were laboratory tap water from Yangzhou University, China. First, 10 mL of tap water samples were collected, and 1000 μL of this sample was added to the supporting electrolyte ($0.1 \text{ mol}\cdot\text{L}^{-1}$ H_2SO_4 -KCl mixed solution ($\text{pH} = 1.0$)); CV was performed under $20 \text{ }^\circ\text{C}$. The current changes at redox peaks were recorded as measurements in the absence or presence of phosphate. The concentrations of phosphate were determined via the standard addition method, and the accuracy was assessed via recovery testing with OCPEs.

Results and discussion

SEM-EDS result of OCPE

Figure 2 shows an $[\text{Omim}]_6\text{Mo}_7\text{O}_{24}$ -carbon paste electrode (OCPE) with Scanning Electron Microscope-Energy Dispersive Spectroscopy (SEM-EDS) acquired at 20.0 kV. We confirm that the OCPE morphology shows flaky clusters on the surface; the $[\text{Omim}]_6\text{Mo}_7\text{O}_{24}$ is well dispersed on the CPE surface.

The XPS spectrum of the OCPE surface layer was carried out after multiple potentiodynamic cycling from -0.4 to 1.2 V in an electrolyte containing phosphate (Fig. 3). The XPS spectrum exhibited a doublet in the Mo 3d electron-binding energy region. Peak i and Peak ii corresponding to Mo 3d appeared as a doublet Mo 3d_{5/2} at 234.93 eV and Mo 3d_{3/2} at 231.85 eV before reacting with phosphate. According to the literature, the binding energy of the peaks (232.5 eV and 235.6 eV) corresponds to the Mo^{6+} state. (Figueredo et al. 2021; Arvas et al. 2019) The corresponding peaks after CV in the presence of H_2PO_4^- also exhibited two resolved peaks at 231.99 eV and 235.15 eV (peaks i' and ii'). The two peaks showed that binding energy 0.65 eV and 0.67 eV were lower than those of Peak i and Peak ii, respectively, which were assigned to Mo 3d_{5/2} and Mo 3d_{3/2} of Mo(V) states in agreement with the data reported in the literature (Sian and Reddy 2004; Maria et al. 2012). There was no indication of Mo (III) and Mo(IV) in the layer deposited on the OCPE surface (appearing at Mo^{4+} (233.09 eV) and Mo^{5+} (234.9 eV) (Figueredo et al. 2021). These results suggest that the parent Mo(VI) surface species convert into Mo(V) upon electroreduction.

Cyclic voltammograms of OCPE

To characterize the electrochemical properties of OCPE for phosphate analysis, an OCPE was subjected to CV in the $0.1 \text{ mol}\cdot\text{L}^{-1}$ H_2SO_4 -KCl mixed solution in the absence or presence of phosphate from -0.4 to 1.2 V

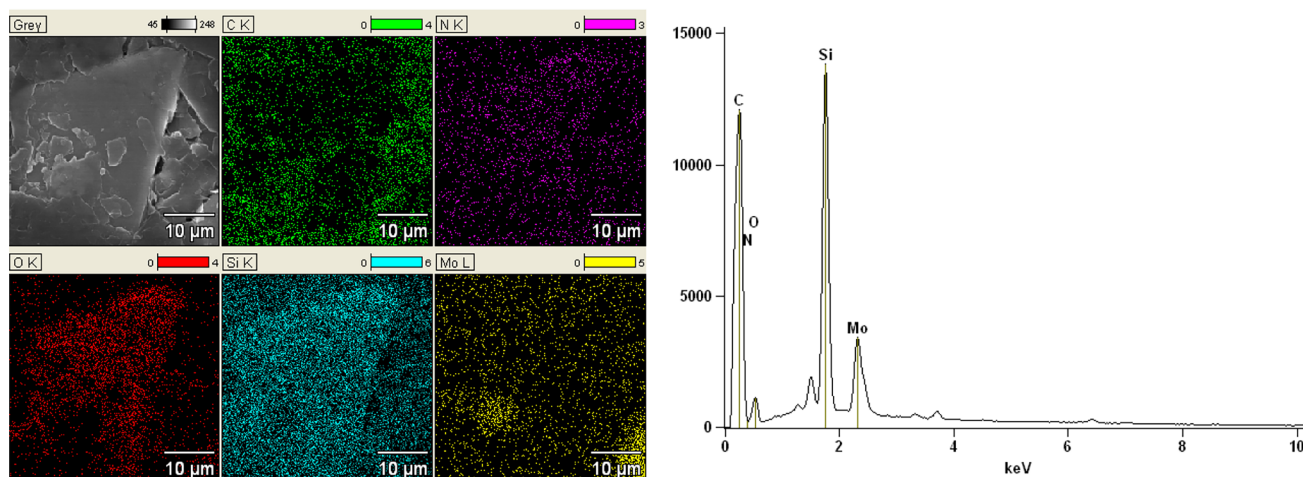


Fig. 2 Scanning Electron Microscope (SEM) images and Energy Dispersive Spectroscopy (EDS) result of OCPE

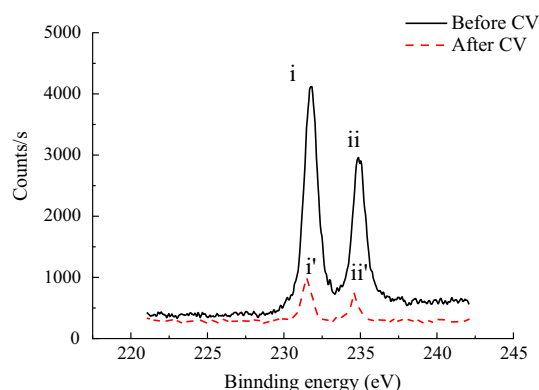


Fig. 3 X-ray Photoelectron Spectroscopy (XPS) analysis of molybdenum species on an OCPE surface

and -0.4 to 0.35 V (Fig. 4). The results are compared with pure GCEs in acidified molybdate (VI) ($0.1 \text{ mol}\cdot\text{L}^{-1} \text{H}_2\text{SO}_4 + 1.0 \text{ mmol}\cdot\text{L}^{-1} \text{MoO}_4^{2-}$) solutions (Fig. 4A). The CV had a very large current response from electroactive polyoxomolybdate substrates due to the enhanced conductivity in the developed OCPE; this material was bulk modified via the uniform dispersion of OCPE in bulky carbons. No clear redox peaks were observed with $[\text{NH}_4]_6\text{Mo}_7\text{O}_{24}$ -CPE due to its pure conductivity (data not shown), while a series of fine redox peaks were found with OCPE.

It is obvious that the substrate current response was much larger with the OCPE than pure CPE (Fig. 4A). While there was a thick background response with OCPE due to the accessible capacitance of the $[\text{O}m]_6\text{Mo}_7\text{O}_{24}$, the resolving power from the peak current was seen by deducting background response and was markedly improved (Liu et al. 2005). The three typical couple peaks C2/A2, C3/A3, and C6/A6 in both potential ranges -0.4 to 1.2 V and -0.2 to 0.36 V (Fig. 4B) show in accordance with literature with

reasonable small peak shifts (Ilangoan and Pillai 1997). It is reasonable by the literature that the three typical couple peaks C2/A2, C3/A3, and C6/A6 in both potential ranges -0.4 – 1.2 V and -0.2 – 0.36 V show small peak shifts (Ilangoan and Pillai 1997).

Comparing Fig. 4A and B, three additional irreversible peaks of A1, A5, and C4 emerge on the OCPE. Note that Fig. 4A voltammograms were obtained under a potential range from -0.4 to 1.2 V. Peak C4 in Fig. 4A is presumably associated with an Mo(VI) reduction according to the following hydrogen molybdenum bronze reactions represented by the general formula H_xMoO_3 where $0 < x \leq 2$ in acid solution. According to literature, Peak C3 is generated from $\text{MoO}_4^{2-} + 4\text{H}^+ + 2\text{e} \rightarrow (\text{H}_2\text{MoO}_3)_{\text{ads}} + \text{H}_2\text{O}$ (Galicia et al. 2011). Then, the anodic peaks of A1, A5, and A7 in Fig. 4A must correspond to the sequence of oxidation of the hydrogen molybdenum bronze $(\text{H}_2\text{MoO}_3)_{\text{ads}}$. This suggests that material dissolved in the solution returns to MoO_4^{2-} according to following reaction ($\text{MoO}_3 + \text{H}_2\text{O} \rightarrow \text{MoO}_4^{2-} + 2\text{H}^+$) along with A1 electrochemical oxidation (Galicia et al. 2011).

Figure 5A shows the plots of peak currents of C2/A2, C3/A3, and C6/A6 versus scan rates. Figure 5B clearly shows that the currents of C2/A2 and C3/A3 were proportional to the scan rate, thus implying that the redox processes are surface-controlled. The C6/A6(C) (Fig. 5C) currents were proportional to the square root of the scan rate, which indicates that the redox process is diffusion controlled.

Optimization of $[\text{Omim}]_6\text{Mo}_7\text{O}_{24}$ percentage to carbon powder

To achieve the best detection sensitivity, the effect of $[\text{Omim}]_6\text{Mo}_7\text{O}_{24}$ percentage on the CV currents was investigated in the $[\text{Omim}]_6\text{Mo}_7\text{O}_{24}$ weight percent range of 0 to

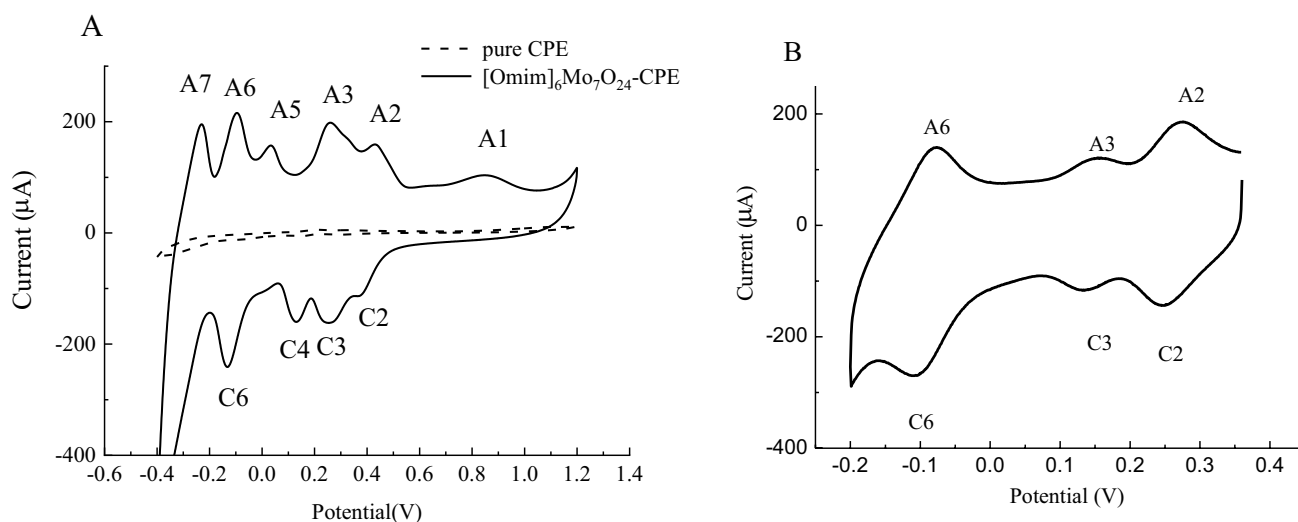


Fig. 4 Cyclic voltammetry (CV) comparative results of OCPE in a solution of $0.1 \text{ mol}\cdot\text{L}^{-1}$ of $\text{KCl}+\text{H}_2\text{SO}_4$ containing 0.010 mM phosphate (solid line) and pure carbon paste electrode (CPE) (dash line) in $1.0 \text{ mmol}\cdot\text{L}^{-1}$ $[\text{NH}_4]_6\text{Mo}_7\text{O}_{24}+0.1 \text{ mol}\cdot\text{L}^{-1}$ of $\text{KCl}-\text{H}_2\text{SO}_4$ solution

at potential ranges of -0.4 to 1.2 V **A**, voltammogram of OCPE at potential ranges of -0.2 to 0.36 V **B**. Scan rates of both CV measurements are 100 mV/s

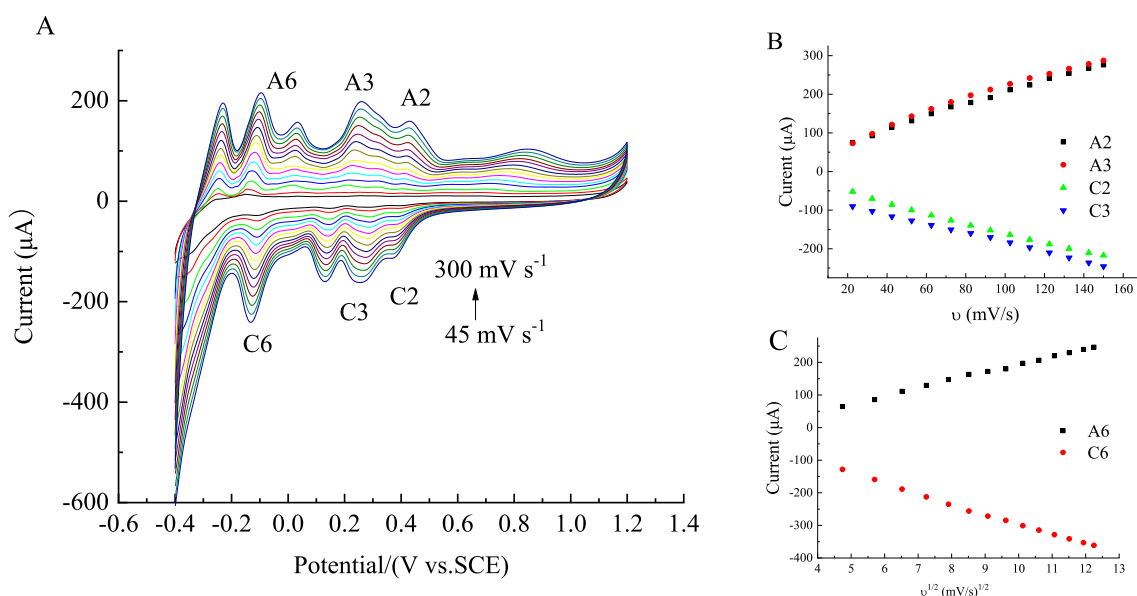


Fig. 5 Voltammograms of OCPE in a solution of $0.1 \text{ mol}\cdot\text{L}^{-1}$ of $\text{H}_2\text{SO}_4\text{-KCl}$ containing $0.010 \text{ mmol}\cdot\text{L}^{-1}$ phosphate at different scan rates **A**; plots of peak currents of C2/A2 and C3/A3 versus scan rates **B**, as well as C6/A6 versus square root of scan rates **C**

20% in a supporting electrolyte solution containing a certain content of H_2PO_4^- from -0.4 to 1.2 V at a scan rate of $100 \text{ mV}\cdot\text{s}^{-1}$ (data not shown). The results showed that CPE with 0% $[\text{Omim}]_6\text{Mo}_7\text{O}_{24}$ does not show any specific redox peaks. However, there were new and obvious redox peaks of kegging ions with 5–20% $[\text{Omim}]_6\text{Mo}_7\text{O}_{24}$ after multiple CV sweeps. The current was highest when the mass ratio of $[\text{Omim}]_6\text{Mo}_7\text{O}_{24}$ was 15%. This mass ratio was selected in all subsequent experiments for the phosphate analysis.

Analytical characteristics

The analytical features of OCPEs were evaluated by CV voltammograms using 1.0×10^{-2} – $1.0 \times 10^{-8} \text{ mol}\cdot\text{L}^{-1}$ standard solutions of phosphate (Fig. 6). According to Randles–Sevcik equation $I_p = kc = 2.69 \times 10^5 n^{3/2} AD^{1/2} v^{1/2} c$, I_p is the peak current (A), n is the number of electron transfers, A is the electrode area (cm^2), D is the diffusion coefficient ($\text{cm}^2\cdot\text{s}^{-1}$), v is the scanning speed ($\text{V}\cdot\text{s}^{-1}$), and c

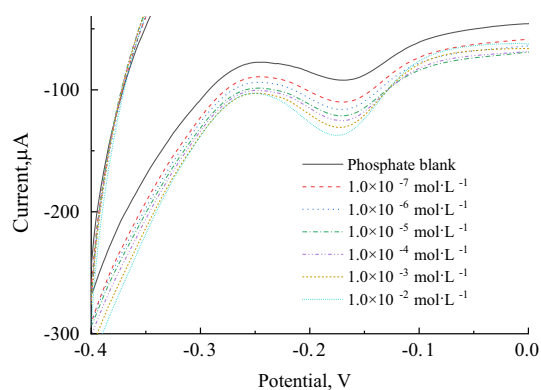


Fig. 6 CV voltammograms of different concentrations of phosphate under an OCPE at a scan rate of $100 \text{ mV}\cdot\text{s}^{-1}$

is the concentration ($\text{mol}\cdot\text{L}^{-1}$). Under optimized experimental conditions, a linear sensing range was obtained between 1.0×10^{-2} and $1.0 \times 10^{-7} \text{ mol}\cdot\text{L}^{-1}$ described by the following equation: $I_p = 5.2657c + 147.212$ ($R^2 = 0.9970$); here, I_p is the current intensity (μA), and c is the H_2PO_4^- concentration ($\text{mol}\cdot\text{L}^{-1}$), sensitivity is $5.3 (\pm 0.1) \mu\text{A}/\mu\text{M}$. The limit of detection ($\text{LOD} = 3\sigma/s$, σ is the slope of linear equation, s is the standard deviation of the detection values for $n=6$ blank samples) was calculated to be $8.5 \times 10^{-8} \text{ mol}\cdot\text{L}^{-1}$.

The analytical conditions, linear range, sensitivity, and LOD of OCPE were compared with previously reported phosphate sensing data (Table 1). The results are comparable with or prior to existing methods (Lu et al. 2021a, b; Shi et al. 2021; Figueredo et al. 2021; Arvas et al. 2019; Sian and Reddy 2004). The resulting LOD value of the proposed method allowed us to select tap water samples to quantitate phosphate concentrations.

Interferences

Interferences from common anions of SO_4^{2-} , Cl^- , HCO_3^- , and NO_3^- were tested, and it was found that they did not interfere with the phosphate quantification. Moreover, the interferences of silicate and glyphosate on the OCPE were

also investigated. Silicate and glyphosate are commonly found in surface waters, and the former is the main interfering substance for the electrochemical determination of phosphate ions (Udman et al. 2005), while the latter is the most widely used herbicide. To study the effect of silicate and glyphosate on OCPE, the concentration of both interfering substances was configured to be 10 times of that phosphate standard solutions, then record the CV current (Fig. 7). The mixed standard solutions of phosphate with sodium silicate have signals that decrease nearly linearly with all phosphate standard solutions ($\text{RSD} = 2.27\%$). These data explain the higher rate constant for the phosphomolybdate complex $[\text{PMo}_{12}\text{O}_{40}]^{3-}$ relative to the silicatemolybdate complex $[\text{SiMo}_{12}\text{O}_{40}]^{4-}$ formation at a chosen pH ($\text{pH} = 1.0$) (Quintana et al. 2004). Therefore, the OCPEs have anti-silicate performance when silicate concentration is tenfold larger than phosphate at the chosen $\text{pH} = 1.0$. Glyphosate did not interfere with OCPE signals under the above experimental

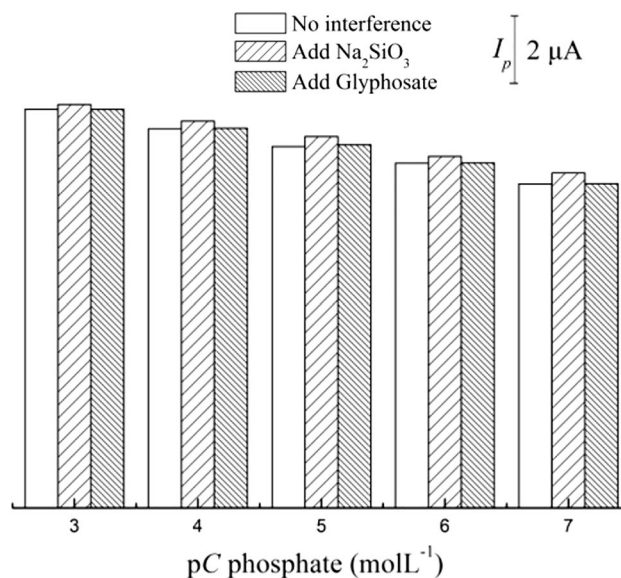


Fig. 7 CV currents for a range of phosphate standards with and without silicate and glyphosate OCPE

Table 1 Comparison of the analytical performances with different electrochemical sensors

Electrode composition	Medium	Detection	LOD/linear range	Sample	Refs.
ZrO ₂ /ZnO/MWCNTs/molybdate/screen printed	H ₂ SO ₄	CV	0.01 μM /0.037–1.1 μM	Soil	Lu et al. (2021a)
Chitosan/Mo ₇ O ₂₄ ⁶⁻	H ₂ SO ₄	CV	0.7 μM /5.0–80 μM	Tap/pond	Lu et al. (2021b)
[N(C ₄ H ₉) ₄] ₄ Mo ₈ O ₂₆ /PE	H ₂ SO ₄	SWV	6.1 nM/1–75 nM	Sea	Shi et al. (2021)
PSS/PEDOT/Chit/Mo ₇ O ₂₄ ⁶⁻	Tris buffer	Amp	ns/0.19–95 μM	n.s	Figueredo et al. (2021)
Molybdenum blue modification	H ₂ SO ₄	DPV	20 nM/0.025–1 μM	Soil	Arvas et al. (2019)
AuNPs/molybdophosphate	H ₂ SO ₄	CV	5.96 μM /0–0.01 mM	Soil	Sian and Reddy (2004)
[Oimim] ₆ Mo ₇ O ₂₄ /Carbon powder	H ₂ SO ₄	CV	85 nM/0.1–10,000 μM	Tap	This work

Table 2 Comparison of recovery values using IC and the proposed methods ($n=3$)

Sample	H_2PO_4^- added, $\mu\text{mol}\cdot\text{L}^{-1}$	IC		OCPE Sensor	
		$[\text{H}_2\text{PO}_4^-] \pm \sigma$ found, $\mu\text{mol}\cdot\text{L}^{-1}$	Recovery range %	$[\text{H}_2\text{PO}_4^-] \pm \sigma$ found, $\mu\text{mol}\cdot\text{L}^{-1}$	Recovery range %
Tap water	0	0.28 ± 0.05	–	0.29 ± 0.02	–
	0.50	0.78 ± 0.04	95.3–105.6	0.80 ± 0.01	100.0–102.5
	0.20	0.49 ± 0.04	94.1–103.3	0.49 ± 0.02	96.8–104.1
	0.10	0.37 ± 0.04	87.5–108.7	0.38 ± 0.03	89.7–105.1

conditions. However, it is not difficult to speculate that organic phosphorus pesticides (OPPs) will have a significant impact on the phosphate determination in the samples with micro-organisms (lake or pond water) which can secrete organic phosphorus hydrolases (OPHs) and convert OPPs to inorganic phosphate.

Determination of phosphate in tap water

The analytical features above were optimized in standard solutions. Then, the suitability of the proposed OCPE system in tap water samples was exploited. Water samples were analyzed using both the proposed and the reference IC method (Table 2). The phosphate concentration was determined to be $0.29 \pm 0.02 \mu\text{mol}\cdot\text{L}^{-1}$ in the tap water sample. This agreed well with that measured by the IC method. To evaluate the accuracy of this sensor, the tap water samples were spiked with a phosphate standard of $10 \mu\text{mol}\cdot\text{L}^{-1}$ leading to satisfactory recovery values comparable to the reference IC method.

The repeatability of the OCPE was evaluated with three sets of H_2PO_4^- detection. The relative standard deviation (RSD) curve slope was 3.5%. The reproducibility of the OCPEs tested with three electrodes and a set of H_2PO_4^- additions obtained from the RSD calibration plot was 4.1%. The storage stability of the electrode was evaluated after seven days of storage at room temperature leading to an RSD of 8.9%.

Conclusions

The $[\text{Omim}]_6\text{Mo}_7\text{O}_{24}$ -based OCPE can effectively retain molybdate in the acidic H_2SO_4 -KCl electrolyte solution. It shows a five-order wide linear range with a high sensitivity for phosphate sensing with relatively simple and low-cost fabrication. The developed CV method with an OCPE could extend to the quantification of phosphate in various samples including environmental and bio-samples.

Acknowledgements This work was supported by Science and Technology Program Nanjing Customs, China (No. 2021KJ21) and Postgraduate Research and Practice Innovation Program of Jiangsu Province (Yangzhou University).

Declarations

Conflict of interest The authors declare no competing interests.

References

- Arvas MB, Gorduk O, Gencten M, Sahin Y (2019) Preparation of a novel electrochemical sensor for phosphate detection based on a molybdenum blue modified poly(vinyl chloride) coated pencil graphite electrode. *Anal Methods* 11:3874. <https://doi.org/10.1039/C9AY01275C>
- Berchmans S, Karthikeyan R, Gupta S, Poinern GEJ, Issa TB, Singh P (2011) Glassy carbon electrode modified with hybrid films containing inorganic molybdate anions trapped in organic matrices of chitosan and ionic liquid for the amperometric sensing of phosphate at neutral pH. *Sens Actuat B* 160:1224–1231. <https://doi.org/10.1016/j.snb.2011.09.052>
- Chang SY, Tseng W-L, Mallipattu S, Chang H-T (2005) Determination of small phosphorus-containing compounds by capillary electrophoresis. *Talanta* 66:411–421. <https://doi.org/10.1016/j.talanta.2004.10.014>
- Cinti S, Talarico D, Palleschi G, Moscone D, Arduini F (2016) Novel reagentless paper-based screen-printed electrochemical sensor to detect phosphate. *Anal Chim Acta* 919:78–84. <https://doi.org/10.1016/j.aca.2016.03.011>
- Clinton-Bailey GS, Grand MM, Beaton AD, Nightingale AM, Owsianka DR, Slavik GJ, Connelly DP, Cardwell CL, Mowlem MC (2017) A lab-on-chip analyzer for in situ measurement of soluble reactive phosphate: improved phosphate blue assay and application to fluvial monitoring. *Environ Sci Technol* 51:9989–9995. <https://doi.org/10.1021/acs.est.7b01581>
- Ellam TJ, Chico TJA (2012) Phosphate: the new cholesterol? The role of the phosphate axis in non-uremic vascular disease. *Atherosclerosis* 220:310–318. <https://doi.org/10.1016/j.atherosclerosis.2011.09.002>
- Figueredo F, Girolametti F, Aneggi E, Lekka M, Annibaldi A, Susmel S (2021) Plastic electrode decorated with polyhedral anion tetrabutylammonium octamolybdate $[\text{N}(\text{C}_4\text{H}_9)_4]_4\text{Mo}_8\text{O}_{26}$ for nM phosphate electrochemical detection. *Anal Chim Acta* 1161:338469. <https://doi.org/10.1016/j.aca.2021.338469>
- Forano C, Farhat H, Mousty C (2018) Recent trends in electrochemical detection of phosphate in actual waters. *Curr Opin Electrochem* 11:55–61. <https://doi.org/10.1016/j.coelec.2018.07.008>
- Galicía A, Zayas T, Salgado L (2011) Voltammetric study of the molybdate reduction and subsequent oxidation on glassy carbon electrode in acid media. *ECS Trans* 36(1):13–19. <https://doi.org/10.1149/1.3660594>
- He G, Zhao L, Chen K, Liu Y, Zhu H (2013) Highly selective and sensitive gold nanoparticle-based colorimetric assay for PO_4^{3-} in aqueous solution. *Talanta* 106:73–78. <https://doi.org/10.1016/j.talanta.2012.11.064>

- Ilangovan G, Pillai KC (1997) Electrochemical and XPS characterization of glassy carbon electrode surface effects on the preparation of a monomeric molybdate(VI)-modified electrode. *Langmuir* 13(3):566–575. <https://doi.org/10.1021/la960053n>
- Kolliopoulos AV, Kampouris DK, Banks CE (2015) Rapid and portable electrochemical quantification of phosphorus. *Anal Chem* 87:4269–4274. <https://doi.org/10.1021/ac504602a>
- Kumar DR, Dhakal G, Nguyen VQ, Lee J, Lee YR, Shim J-J (2021) Ammonium heptamolybdate preloaded on flexible carbon-matrix film electrode for the electrochemical phosphate sensor in a river water sample. *Microchem J* 170:106639. <https://doi.org/10.1016/j.microc.2021.106639>
- Liu H, He P, Li Z, Sun C, Shi L, Liu Y, Zhu G, Li J (2005) An ionic liquid-type carbon paste electrode and its polyoxometalate-modified properties. *Electrochim Commun* 7:1357–1363. <https://doi.org/10.1016/j.elecom.2005.09.018>
- Liu W, Du Z, Qian Y, Li F (2013) A specific colorimetric probe for phosphate detection based on anti-aggregation of gold nanoparticles. *Sensor Actuat B* 176:927–931. <https://doi.org/10.1016/j.snb.2012.10.074>
- Lu Y, Lan Q, Zhang C, Liu B, Wang X, Xu X, Liang X (2021a) Trace-level sensing of phosphate for natural soils by a nanoscreen-printed electrode. *Environ Sci Technol* 55(19):13093–13102. <https://doi.org/10.1021/acs.est.1c05363>
- Lu Y, Li X, Li D, Compton RG (2021b) Amperometric environmental phosphate sensors. *ACS Sens* 6:3284–3294. <https://doi.org/10.1021/acssensors.1c01035>
- Macintosh KA, Mayer BK, McDowell RW, Powers SM, Baker LA, Boyer TH, Rittmann BE (2018) Managing diffuse phosphorus at the source versus at the sink. *Environ Sci Technol* 52:11995–12009. <https://doi.org/10.1021/acs.est.8b01143>
- Maria B-B, Tomasz W, Teresa Ł, Józef C (2012) Catalytic effect of molybdenum oxo-species on reduction of allyl alcohol at a Pt electrode in strongly acidic solutions. *Electrochim Acta* 63:89–99. <https://doi.org/10.1016/j.electacta.2011.12.081>
- Nagaraj K, Nityananda SA, Darshak RT (2021) Recent advances in the fluorescent and colorimetric detection of dihydrogen phosphate. *Supramol Chem* 33(8):408–441. <https://doi.org/10.1080/10610278.2022.2035387>
- Nagul EA, McKelvie ID, Worsfold P, Kolev SD (2015) The molybdenum blue reaction for the determination of orthophosphate revisited: opening the black box. *Anal Chim Acta* 890:60. <https://doi.org/10.1016/j.aca.2015.07.030>
- Quintana JC, Idrissi L, Palleschi G, Albertano P, Armine A, El Rhazi M, Moscone D (2004) Investigation of amperometric detection of phosphate: Application in seawater and cyanobacterial biofilm samples. *Talanta* 63:567–574. <https://doi.org/10.1016/j.talanta.2003.11.040>
- Ruiz-Calero V, Galceran MT (2005) Ion chromatographic separations of phosphorus species: a review. *Talanta* 66:376–410. <https://doi.org/10.1016/j.talanta.2005.01.027>
- Shi J, Guo Z, Tian S, Li M (2021), Determination of PF6⁻ in environmental water by [Omim]₆Mo₇O₂₄ carbon paste ion selective electrode (in Chinese). *PTCA (Part B: Chem Anal)* 57:193. <https://doi.org/10.11973/lhgy-hx202103001>
- Sian TS, Reddy GB (2004) Optical, structural and photoelectron spectroscopic studies on amorphous and crystalline molybdenum oxide thin films. *Sol Energy Mater Sol Cells* 82:375–386. <https://doi.org/10.1016/j.solmat.2003.12.007>
- Snigur D, Chebotarev A, Bulat K, Duboviy V (2020) Fast room temperature cloud point extraction procedure for spectrophotometric determination of phosphate in water samples. *Anal Biochem* 597:113671. <https://doi.org/10.1016/j.ab.2020.113671>
- Talarico D, Cinti S, Arduini F, Amine A, Moscone D, Palleschi G (2015) Phosphate detection through a cost-effective carbon black nanoparticle-modified screen-printed electrode embedded in a continuous flow system. *Environ Sci Technol* 49:7934–7939. <https://doi.org/10.1021/acs.est.5b00218>
- Udman Y, McKelvie ID, Grace MR, Jakmunee J, Grudpan K (2005) Evaluation of on-line preconcentration and flow-injection amperometry for phosphate determination in fresh and marine waters. *Talanta* 66(2):461–466. <https://doi.org/10.1016/j.talanta.2004.12.064>
- Yan JC, Ren J, Ren LL, Jian J, Yang Y, Yang SF, Ren TL (2019) Development of a portable setup using a miniaturized and high precision colorimeter for the estimation of phosphate in natural water. *Anal Chim Acta* 1058:70–79. <https://doi.org/10.1016/j.aca.2019.01.030>
- Zhang Z, Tao H, Cao Q, Li L, Xu S, Li Y, Liu Y (2022) Ratiometric fluorescence sensor for sensitive detection of inorganic phosphate in environmental samples. *Anal Bioanal Chem* 414:3507–3515. <https://doi.org/10.1007/S00216-022-03973-0>

Publisher's Note Springer Nature remains neutral with regard to jurisdictional claims in published maps and institutional affiliations.

Springer Nature or its licensor (e.g. a society or other partner) holds exclusive rights to this article under a publishing agreement with the author(s) or other rightsholder(s); author self-archiving of the accepted manuscript version of this article is solely governed by the terms of such publishing agreement and applicable law.